

The autoparametric 3:2 resonance in conservative systems

JIŘÍ HORÁK

Astronomical Institute, The Czech Academy of Sciences, Boční II, CZ-140 31 Prague, Czech Republic

Received; accepted; published online

Abstract. In the resonance model, high-frequency quasi-periodic oscillations (QPOs) are supposed to be a consequence of nonlinear resonance between modes of oscillations occurring within the innermost parts of an accretion disk. Several models with a prescribed mode–mode interaction were proposed in order to explain the characteristic properties of the resonance in QPO sources. In this paper, we examine nonlinear oscillations of a system having two degrees of freedom and we show that this case could be particularly relevant for QPOs. We present a very convenient way how to study autoparametric resonances of a fully general system using the method of multiple scales. We concentrate to conservative systems and discuss their behavior near the 3:2 parametric resonance.

Key words: nonlinear resonance, perturbation methods, multiple scales

©0000 WILEY-VCH Verlag GmbH & Co. KGaA, Weinheim

1. Introduction

In the resonance model (Abramowicz & Kluźniak 2001; Kluźniak & Abramowicz 2000; Kato 2003), there is a natural and attractive possibility of explaining the observed rational ratios of high-frequency QPOs as a consequence of nonlinear coupling between different modes of accretion disk oscillations. The idea has been pursued in several papers (recently, e.g. Abramowicz et al. 2003; Rebusco 2004).

Specific models invoke particular physical mechanisms. Some models can be almost immediately comprehended as distinct realizations of the general approach discussed here – for example, various formulations of the orbiting spot model (Schnittman & Bertchinger 2004) or the models, where QPOs are produced by the magnetically driven resonance in a diamagnetic accretion disk (Lai 1999) – while other seem to be more distant from the view presented herein – e.g. the transition layer model (Titarchuk 2002), an interesting idea of p-mode oscillations of a small accretion torus (Rezzola et al. 2003) or the model of blobs in an accretion disc (see e.g. Karas 1999; Li & Narayan 2004, and references cited therein). Also in this context, Kato (2004) discussed the resonant interaction between waves propagating in a warped disk, including their rigorous mathematical description. Instead of pursuing a specific model, here we keep the discussion as general as possible, aiming to implement the formalism of multiple scales. Indeed, we show that there is unques-

tionable appeal in this approach which offers some additional insight into generic properties of resonant oscillations.

Some properties of an accretion disk oscillations can be discussed within the epicyclic approximation of a test particle on a circular orbit near equatorial plane. Suppose that angular momentum of the particle is fixed to a value ℓ . The effective potential $U_\ell(r, \theta)$ has a minimum at radius r_0 , corresponding to the location of the stable circular orbit. An observer moving along this orbit measures radial, vertical and azimuthal epicyclic oscillations of a particle nearby. Since the angular momentum of the particle is conserved, only two of them – radial and vertical – are independent. The epicyclic frequencies can be derived from the geodesic equations expanded to the linear order in deviations $\delta r = r - r_0$ and $\delta \theta = \theta - \pi/2$ from the circular orbit. We get two independent second-order differential equations describing two uncoupled oscillators with frequencies ω_r and ω_θ , which are given by the second derivatives of effective potential $U_\ell(r, \theta)$.

In Newtonian theory, ω_r and ω_θ are equal to the Keplerian orbital frequency Ω_K . This is in tune with the fact that orbits of particles are planar and closed curves. The degeneracy between two epicyclic frequencies can be seen as a result of scale-freedom of the Newtonian gravitational potential (Abramowicz & Kluźniak 2003). In Schwarzschild geometry this freedom is broken by introducing the gravitational radius $r_g = 2GM/c^2$. The degeneracy between the vertical epicyclic and the orbital frequencies is related to spherical symmetry of the gravitational potential, which assures the

existence of planar trajectories of particles. All three frequencies are different in the vicinity of a rotating Kerr black hole.

In addition, when nonlinear terms of geodesic equations are included, the two oscillations in r and θ directions become coupled and variety of new phenomena connected to nonlinear nature of the equations appear. This rich phenomenology includes frequency shift of observed frequencies with respect to eigenfrequencies, presence of higher harmonics and subharmonics, drifts and parametric resonance. The first three are connected to nonlinear oscillations of each mode and the last one comes from the coupling between two modes.

2. Expansion via multiple scales

We study nonlinear oscillations of the system having two degrees of freedom, i.e., the coordinate perturbations δr and $\delta\theta$. The oscillations are described by two coupled differential equations of the very general form

$$\ddot{\delta r} + \omega_r^2 \delta r = \omega_r^2 f_r(\delta r, \delta\theta, \dot{\delta r}, \dot{\delta\theta}), \quad (1)$$

$$\ddot{\delta\theta} + \omega_\theta^2 \delta\theta = \omega_\theta^2 f_\theta(\delta r, \delta\theta, \dot{\delta r}, \dot{\delta\theta}). \quad (2)$$

Suppose that the functions f_r and f_θ are nonlinear, i.e., their Taylor expansions start in the second order. Our another assumption is that these functions are invariant under reflection of time (i.e., the Taylor expansion does not contain odd powers of time derivatives of δr and $\delta\theta$). As we shall see later, this is related to the conservation of the total energy in the system. Many authors studied such systems with a particular form of functions f and g (Nayfeh & Mook 1979), however, in this paper we keep the discussion fully general.

We seek the solutions of the governing equations in the form of the multiple-scales expansions (Nayfeh & Mook 1979)

$$\delta r(t, \epsilon) = \sum_{n=1}^4 \epsilon^n r_n(T_\mu), \quad \delta\theta(t, \epsilon) = \sum_{n=1}^4 \epsilon^n \theta_n(T_\mu), \quad (3)$$

where several time scales T_μ are introduced instead of the physical time t ,

$$T_\mu \equiv \epsilon^\mu t, \quad \mu = 0, 1, 2, 3. \quad (4)$$

The time scales are treated as independent. It follows that instead of the single time derivative we have an expansion of partial derivatives with respect to the T_μ

$$\frac{d}{dt} = D_0 + \epsilon D_1 + \epsilon^2 D_2 + \epsilon^3 D_3 + \mathcal{O}(\epsilon^4), \quad (5)$$

$$\frac{d^2}{dt^2} = D_0^2 + 2\epsilon D_0 D_1 + \epsilon^2 (D_1^2 + 2D_0 D_2) + 2\epsilon^3 (D_0 D_3 + D_1 D_2) + \mathcal{O}(\epsilon^4), \quad (6)$$

where $D_\mu = \partial/\partial T_\mu$.

We expand the nonlinear functions f_r and f_θ into the Taylor series and then we substitute the expansions (3), (5) and (6). Finally, we compare the coefficients of the same powers of ϵ on both sides in the resulting couple of equations. This way we get a set of *linear* second-order differential equations that can be solved successively – the lower-order terms of the

expansion (3) appear as forcing terms on the right-hand sides of the equations for the higher order approximations.

In the first order we obtain equations corresponding to the linear approximation

$$(D_0^2 + \omega_r^2)r_1 = 0, \quad (D_0^2 + \omega_\theta^2)\theta_1 = 0. \quad (7)$$

with the solutions

$$x_1 = A_r(T_1, T_2, T_3)e^{i\omega_r T_0} + \text{cc}, \quad (8)$$

$$\theta_1 = A_\theta(T_1, T_2, T_3)e^{i\omega_\theta T_0} + \text{cc}. \quad (9)$$

The complex amplitudes \hat{A}_r and A_θ generally depend on the higher time-scales.

The solutions (8) and (9) substituted into the quadratic terms on the right-hand sides of the second-order differential equations produce terms that oscillates with frequencies $2\omega_r$, $2\omega_\theta$ and $\omega_\theta \pm \omega_r$. When the frequency ratio ω_r/ω_θ is far from 1:2 and 2:1 the particular solutions r_2 and θ_2 describe higher harmonics to the linear-order oscillations r_1 and θ_1 . Hence, the presence of higher harmonics in the power-spectra is a signature of nonlinear oscillations. Their frequencies and relative strengths with respect to the main oscillations provide us an usefull informations about nonlinearities in the system.

In addition, the right hand sides of the second order equations contain terms proportional to $e^{i\omega_r T_0}$ and $e^{i\omega_\theta T_0}$ that oscillates with the same frequency as the eigenfrequency of the oscillators. These terms produces secular grow of the amplitudes of the second-order approximations r_2 and θ_2 and causes nonuniform expansions (3). Eliminating them we get the *solvability conditions* for the complex amplitudes $A_r(T_1, T_2, T_3)$ and $A_\theta(T_1, T_2, T_3)$ that give us the evolution of the system on longer time-scales (Nayfeh & Mook 1979).

When the eigenfrequencies are in 1:2 or 2:1 ratio we observe qualitatively different behavior related to the *autoparametric resonance*. In that case the right hand sides contains additional secular terms and the solvability conditions take different form. Different resonances occur in different orders of approximation. The possible resonances in the third order are 1:3, 1:1 and 3:1 and 1:4, 3:2, 2:3 and 4:1 in the fourth order¹ However, if the governing equations remain unchanged under the transformation $\delta\theta \rightarrow -\delta\theta$ (i.e., the system is reflection symmetric) the only autoparametric resonances that exists in the system are 1:2, 1:1, 1:4 and 3:2 (Rebusco 2004)

3. The 3:2 autoparametric resonance

Let us consider oscillations of a conservative system eigenfrequencies of which are close to 3:2. The time behavior of the observed frequencies ω_r^* and ω_θ^* and amplitudes a_r and a_θ of the oscillations can be found from the solvability conditions imposed on the complex amplitudes $A_r(T_1, T_2, T_3)$ and $A_\theta(T_1, T_2, T_3)$ (Horák et al. 2005)

$$D_1 A_r = D_2 A_\theta = 0, \quad (10)$$

$$D_2 A_r = -\frac{i\omega_r}{2} [\kappa_r |A_r|^2 + \kappa_\theta |A_\theta|^2] A_r, \quad (11)$$

$$D_2 A_\theta = -\frac{i\omega_\theta}{2} [\lambda_r |A_r|^2 + \lambda_\theta |A_\theta|^2] A_\theta, \quad (12)$$

¹ The ratio $n : m$ refers to the eigenfrequency ratio $\omega_\theta : \omega_r$.

$$D_3 A_r = -\frac{i}{2} \omega_r \alpha (A_r^2)^* A_\theta^2 e^{-i(\sigma_2 T_2 + \sigma_3 T_3)}, \quad (13)$$

$$D_3 A_\theta = -\frac{i}{2} \omega_\theta \beta A_r^3 A_\theta^* e^{i(\sigma_2 T_2 + \sigma_3 T_3)}. \quad (14)$$

In the fourth order we eliminate also terms which become secular in when $3\omega_r \approx 2\omega_\theta$. We describe vicinity of the resonance by the detuning parameters σ_2 and σ_3 introduced according to

$$3\omega_r = 2\omega_\theta + \epsilon^2 \sigma_2 + \epsilon^3 \sigma_3. \quad (15)$$

The term $\epsilon \sigma_1$ is missing, because the complex amplitudes depends only on the second and the third time-scales. The solvability conditions describe evolution of the system in the most general way: the real parameters α , β , κ_r , κ_θ , λ_r and λ_θ are given by the coefficients of the Taylor-expanded nonlinear functions f_r and f_θ .

Since A_r and A_θ are complex, the conditions (10)–(14) represents 12 real equations. However few of them are trivial. By substituting the polar forms $\epsilon A_r = \frac{1}{2} a_r e^{i\phi_r}$ and $\epsilon A_\theta = \frac{1}{2} a_\theta e^{i\phi_\theta}$, separating real and imaginary parts and introducing the unique time t the number of the equations can be reduced to four,

$$\dot{a}_\rho = \frac{\alpha \omega_r}{16} a_\rho^2 a_\theta^2 \sin \gamma, \quad (16)$$

$$\dot{a}_\theta = -\frac{\beta \omega_\theta}{16} a_\rho^3 a_\theta \sin \gamma, \quad (17)$$

$$\dot{\phi}_\rho = -\frac{\omega_r}{2} [\kappa_r a_\rho^2 + \kappa_\theta a_\theta^2] - \frac{\alpha \omega_r}{16} a_\rho a_\theta^2 \cos \gamma, \quad (18)$$

$$\dot{\phi}_\theta = -\frac{\omega_\theta}{2} [\lambda_r a_\rho^2 + \lambda_\theta a_\theta^2] - \frac{\beta \omega_\theta}{16} a_\rho^3 \cos \gamma, \quad (19)$$

where we introduced the phase function $\gamma(t) = 2\phi_\theta(t) - 3\phi_r(t) - \sigma t$ and the unique detuning parameter $\sigma = \epsilon^2 \sigma_2 + \epsilon^3 \sigma_3$. The equations (16) and (17) describes the slow evolution of the amplitudes of oscillations and additional long-term behavior of the oscillation phases is given by equations (18) and (19). These equations give us the frequency-shift of the observed frequencies ω_r^* and ω_θ^* with respect to the eigenfrequencies ω_r and ω_θ , respectively,

$$\omega_r^* = \omega_r + \dot{\phi}_r, \quad \omega_\theta^* = \omega_\theta + \dot{\phi}_\theta. \quad (20)$$

The two equations (18) and (19) can be replaced by a single differential equation for the phase function,

$$\dot{\gamma} = -\sigma + \frac{\omega_\theta}{4} \left[\mu_r a_r^2 + \mu_\theta a_\theta^2 + \frac{a_r}{2} (\alpha a_\theta^2 - \beta a_r^2) \cos \gamma \right], \quad (21)$$

where we used the fact that near the resonance $\omega_r \approx (2/3)\omega_\theta$ and we defined $\mu_r = \kappa_r - \lambda_r$ and $\mu_\theta = \kappa_\theta - \lambda_\theta$.

3.1. Steady-state solutions

Steady-state solutions are characterized by constant amplitudes and frequencies of oscillations. Such solutions represent singular points of the system governed by equations (16), (17) and (21).

It is obvious from equations (16) and (17) that the condition $\dot{a}_r = \dot{a}_\theta = 0$ can be satisfied (with nonzero amplitudes) only if $\sin \gamma = 0$ (identically at all times), and thus also $\dot{\gamma} = 0$. In that case equation (21) transforms to the algebraic equation

$$\frac{\sigma}{\omega_\theta} = \frac{1}{4} \left[\mu_r a_r^2 + \mu_\theta a_\theta^2 \pm \frac{a_r}{2} (\alpha a_\theta^2 - \beta a_r^2) \right]. \quad (22)$$

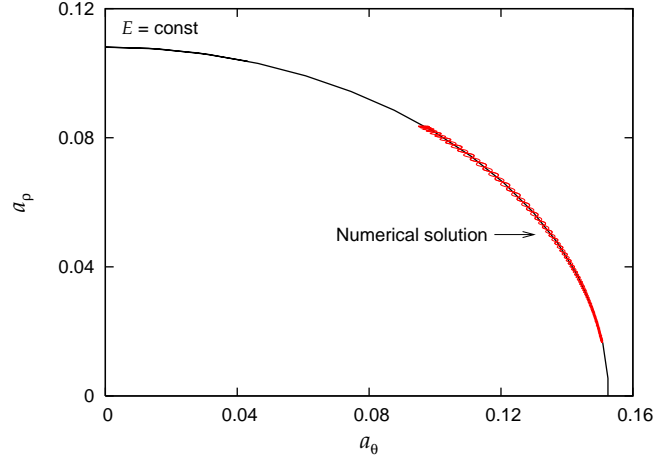


Fig. 1. Comparison between an analytical constraint (27) and the corresponding numerical solution of the system Abramowicz et al. (2003). Each point corresponds to the amplitudes of the oscillations at a particular time. On the other hand, from the discussion of equation (27) we know that these points must lay on an ellipse, whose shape is determined by the multiple-scales method.

The left-hand side can be expressed using the eigenfrequency ratio $R = \omega_\theta / \omega_r$ as

$$\frac{\sigma}{\omega_\theta} = -\frac{2}{R} \left(R - \frac{3}{2} \right). \quad (23)$$

Then we get

$$R = \frac{3}{2} - \frac{3}{16} (\mu_r a_r^2 + \mu_\theta a_\theta^2) \pm \frac{3}{32} a_r (\alpha a_\theta^2 - \beta a_r^2), \quad (24)$$

where we neglected terms of the fourth order. Note that the lowest correction to eigenfrequencies is of the second order – for given amplitudes a_r , a_θ the steady-state oscillations occur when the eigenfrequency ratio departs from 3/2 by deviation of order of a^2 .

The relation between observed frequencies of oscillations ω_r^* , ω_θ^* and eigenfrequencies ω_r , ω_θ are given by the time derivative of phases ϕ_r and ϕ_θ . We can find simple relation between observed frequencies and the phase function

$$\begin{aligned} 3\omega_r^* - 2\omega_\theta^* &= 3\omega_r - 2\omega_\theta + (3\dot{\phi}_r - 2\dot{\phi}_\theta) \\ &= \sigma + (3\dot{\phi}_r - 2\dot{\phi}_\theta) = -\dot{\gamma}. \end{aligned} \quad (25)$$

For steady state solutions $\dot{\gamma} = 0$, and thus observed frequencies are adjusted to *exact* 3:2 ratio even if eigenfrequencies depart from it.

3.2. Integrals of motion

The method of investigation of time-dependent behavior of the system is analogical to the case of 1:2 resonance as examined by Nayfeh & Mook (1979). The oscillations are described by three variables $a_r(t)$, $a_\theta(t)$ and $\gamma(t)$ and three first-order differential equations (16), (17) and (21). However, the number of differential equations can be reduced to one because it is possible to find two integrals of motion. Our discussion will be

Consider equations (16) and (17). Eliminating $\sin \gamma$ from both equations we find

$$\frac{d}{dt}(a_r^2 + \nu a_\theta^2) = 0 \quad (26)$$

and thus

$$a_r^2 + \nu a_\theta^2 = \text{const} \equiv E, \quad (27)$$

where we defined

$$\nu = \frac{\alpha \omega_r}{\beta \omega_\theta} \approx \frac{2\alpha}{3\beta}. \quad (28)$$

When $\nu > 0$, the both amplitudes of oscillations are bounded. The curve $[a_r(t), a_\theta(t)]$ is a segment of an ellipse. The constant E is proportional to the energy of the system. On the other hand, when $\nu < 0$, one amplitude of oscillations can grow without bounds while the second amplitude vanishes. This case corresponds to the presence of an regenerative element in the system (Nayfeh & Mook 1979). The corresponding curve in the (a_r, a_θ) plane is a hyperbola. In further discussion we assume that $\nu > 0$.

In order to verify that the the energy of the system is conserved, we numerically integrated governing equation (1) and (2) for the one particular system discussed by Abramowicz et al. (2003). The comparison is in Figure 1. The numerical and analytical results are in a very good agreement.

The second integral of motion is found in following way. Let us multiply equation (21) by a_θ . Then we obtain

$$a_\theta \dot{\gamma} = -\sigma a_\theta + \frac{\omega_\theta}{4} \mu_r a_r^2 a_\theta + \frac{\omega_\theta}{4} \mu_\theta a_\theta^3 + \frac{\omega_\theta}{8} \alpha a_r a_\theta^3 \cos \gamma - \frac{\omega_\theta}{8} \beta a_r^3 a_\theta \cos \gamma. \quad (29)$$

Changing the independent variable from t to a_θ and multiplying the whole equation by da_θ we find

$$a_r^3 a_\theta^2 d(\cos \gamma) + \frac{8\sigma}{\beta \omega_\theta} d(a_\theta^2) - \frac{4\mu_r}{\beta} a_r^2 a_\theta d(a_\theta^2) - \frac{\mu_\theta}{\beta} d(a_\theta^4) - \frac{2\alpha}{\beta} a_r a_\theta^3 \cos \gamma da_\theta + 2a_r^3 a_\theta \cos \gamma da_\theta = 0. \quad (30)$$

The equation (27) implies

$$a_\theta da_\theta = -\frac{a_r da_r}{\nu}. \quad (31)$$

With the aid of this relation equation (30) takes the form

$$3a_r^2 a_\theta^2 \cos \gamma da_r + 2a_r^3 a_\theta \cos \gamma da_\theta + a_r^3 a_\theta^2 d(\cos \gamma) + \frac{8\sigma}{\beta \omega_\theta} d(a_\theta^2) + \frac{\mu_r}{\beta \nu} d(a_r^4) - \frac{\mu_\theta}{\beta} d(a_\theta^4) = 0. \quad (32)$$

The first three terms express the total differential of function $-a_r^3 a_\theta^2 \cos \gamma$. Hence, the above equation can be arranged to the form

$$d\left(a_r^3 a_\theta^2 \cos \gamma + \frac{8\sigma}{\beta \omega_\theta} a_\theta^2 + \frac{\mu_r}{\beta \nu} a_r^4 - \frac{\mu_\theta}{\beta} a_\theta^4\right) = 0. \quad (33)$$

In other words,

$$a_r^3 a_\theta^2 \cos \gamma + \frac{8\sigma}{\beta \omega_\theta} a_\theta^2 + \frac{\mu_r}{\beta \nu} a_r^4 - \frac{\mu_\theta}{\beta} a_\theta^4 = \text{const} \equiv L \quad (34)$$

is another integral of equations (16), (17) and (21).

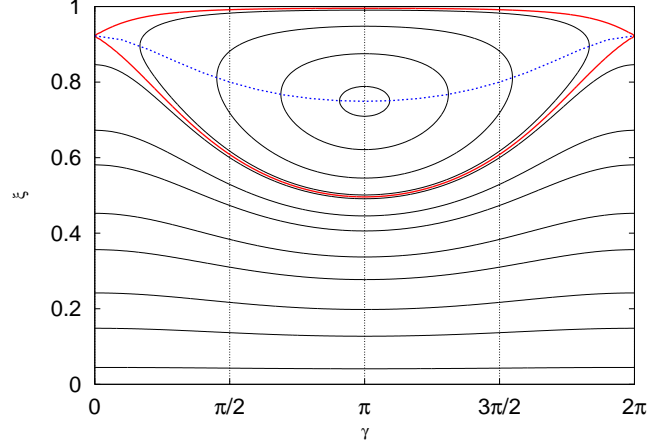


Fig. 2. Example of the (γ, ξ) -plane for the system close to the 3:2 resonance. The oscillations are coupled by nonlinear functions f_ρ and f_θ [see equations (1) and (2)]. These functions give us values of the constants α , β , κ_r , κ_θ , λ_r and λ_θ . The thick solid line is the separatrix dividing the librating and circulating trajectories. The blue dotted line connects points where $\dot{\gamma} = 0$. The example is for values $\alpha = \beta = \kappa_r = \lambda_\theta = 1$, $\kappa_\theta = \lambda_\theta = 2$, $\mathcal{E} = 0.1$ and $\sigma = -0.165$.

3.3. Analytical results

Knowing two integrals of motion, we are able to find one differential equation which governs the time-evolution of the system.

First, the amplitudes a_r and a_θ are not independent because they are related by equation (27). To satisfy this relation, let us define new variable $\xi(t)$ by

$$a_r^2 = \xi E, \quad a_\theta^2 = (1 - \xi) \frac{E}{\nu}. \quad (35)$$

For present moment, we ignore the time dependence by considering projections of solutions into the (γ, ξ) -plane. For a fixed energy E of oscillations, the system follows curves of constant L . Hence, the trajectories in the (γ, ξ) -plane are given by equation

$$L(\gamma, \xi) = \text{const}. \quad (36)$$

An example of the phase-plane is given in Figure 2. There are two types of trajectories $[\xi(t), \gamma(t)]$: the *circulating* trajectories take the full range $0 \leq \gamma(t) \leq 2\pi$ and the *librating* trajectories that are confined in the smaller range $\gamma_1 \leq \gamma(t) \leq \gamma_2$. The turning points on the librating trajectories correspond to $\gamma = \gamma_1$ and $\gamma = \gamma_2$. This division has an interesting consequences with respect to the observed frequencies of resonant oscillations. According to the relation (25) the observed frequencies are in exact 3:2 ratio when the system pass through these points. On the other hand, the circulating trajectories do not contain any turning points and the ratio of observed frequencies is always above or below 3:2.

The equation describing the evolution of $\xi(t)$ can be derived in the following way. Let us multiply equation (16) by $2a_r$ and integrate it. We obtain

$$\frac{d(a_r^2)}{dt} = \frac{\alpha}{8} \omega_r a_r^3 a_\theta^2 \sin \gamma. \quad (37)$$

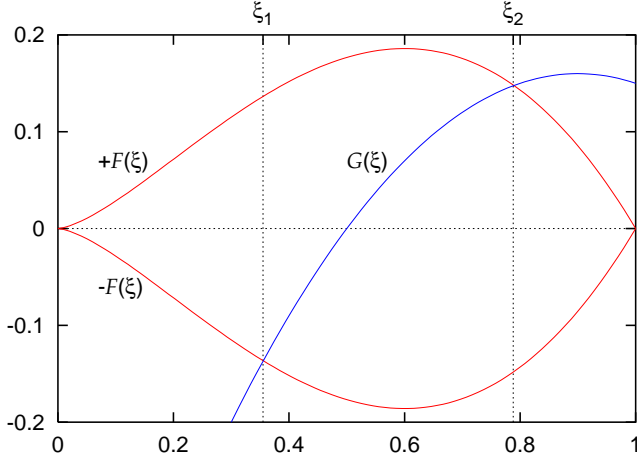


Fig. 3. The functions $\pm F(\xi) = \pm(1 - \xi)\xi^{3/2}$ and the quadratic function $G(\xi)$ whose second powers are first and second terms on the right-hand side of equation (40). The behavior of the system corresponds to ξ in the interval $[\xi_1, \xi_2]$ (denoted by the two dotted vertical lines) where the condition $|F(\xi)| \geq |G(\xi)|$ is satisfied.

Then we express a_r^2 using ξ , and square it. We find

$$\left(\frac{8E}{\alpha\omega_r}\right)^2 \xi^2 = (a_r^3 a_\theta^2 \sin \gamma)^2. \quad (38)$$

The right-hand side of this equation can be expressed using equation (34) as

$$(a_r^3 a_\theta^2 \sin \gamma)^2 = (a_r^3 a_\theta^2)^2 - \left(L - \frac{8\sigma}{\beta\omega_\theta} a_\theta^2 - \frac{\mu_r}{\beta\nu} a_r^4 + \frac{\mu_\theta}{\beta} a_\theta^4\right)^2. \quad (39)$$

After the substitution into equation (38) and using the relations (35), we get

$$\frac{1}{E^3} \left(\frac{8}{\beta\omega_\theta}\right)^2 \xi^2 = (1 - \xi)^2 \xi^3 - \frac{\nu^2}{E^5} \left[L - \frac{8\sigma E}{\beta\nu\omega_\theta} (1 - \xi) - \frac{\mu_r E^2}{\beta\nu} \xi^2 + \frac{\mu_\theta E^2}{\beta\nu^2} (1 - \xi)^2 \right]^2. \quad (40)$$

The equation of motion has a form

$$\mathcal{K}^2 \dot{\xi}^2 = F^2(\xi) - G^2(\xi), \quad (41)$$

where the \mathcal{K}^2 is a positive constant, $F(\xi) = (1 - \xi)\xi^{3/2}$ and $G(\xi)$ is a quadratic function coefficients of which depend on initial conditions through E and L . The motion occurs only for ξ that satisfy $|F(\xi)| \geq |G(\xi)|$. The turning points, where $\dot{\xi}$ changes its signature, are determined by the condition

$$|F(\xi)| = |G(\xi)|. \quad (42)$$

The functions $\pm F(\xi)$ and $G(\xi)$ are plotted in Figure 3. Generally, the function G intersects the functions $\pm F$ in two points that corresponds to $\xi(t)$ oscillating between the two bounds ξ_1 and ξ_2 given by condition (42). The radial and vertical mode of oscillations periodically exchanges the energy. The amount of exchanged energy is given by $\Delta E/E =$

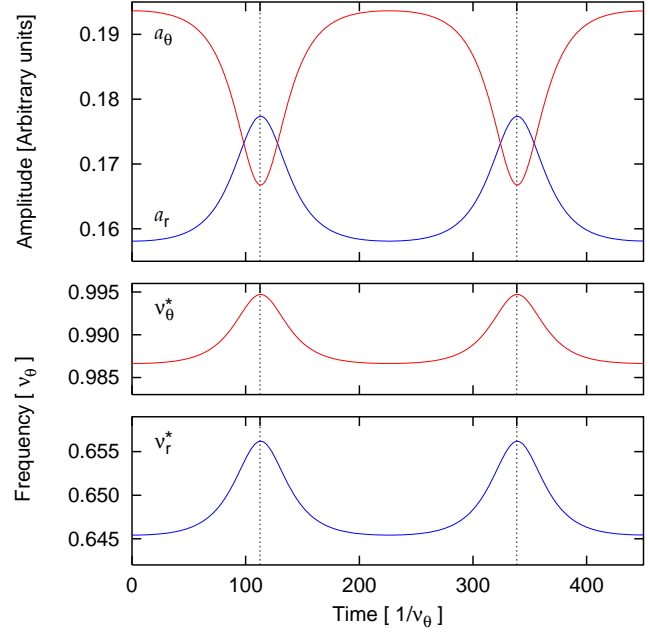


Fig. 4. Time evolution of the amplitudes (top panel) and the observed frequencies, $\nu_\theta^* = \omega_\theta^*/(2\pi)$ (middle panel) and $\nu_r^* = \omega_r^*/(2\pi)$ (bottom panel). All quantities are rescaled with respect to the higher eigenfrequency ν_θ . Amplitudes of the oscillations are anticorrelated because the energy is conserved. Observed frequencies are correlated because the system is in parametric resonance.

$\xi_2 - \xi_1$. For some particular values of L and E only one intersection of $\pm F$ and G exists (the function $G(\xi)$ touch one of the functions $\pm F(\xi)$)— the oscillations of the system correspond to the steady-state solutions discussed above.

The period of the energy exchange can be find by integration of equation (40)

$$T = \frac{16}{\beta\omega_\theta} E^{-3/2} \int_{\xi_1}^{\xi_2} \frac{d\xi}{\sqrt{F^2(\xi) - G^2(\xi)}}. \quad (43)$$

This integral can be roughly approximated as

$$T \sim \frac{16\pi}{\beta\omega_\theta} E^{-3/2}. \quad (44)$$

However, near the steady state the period becomes much longer.

The observed frequencies ω_r^* and ω_θ^* are given by relations (25). They depend on squared amplitudes a_r^2 and a_θ^2 . Since both a_r^2 and a_θ^2 depend linearly on $\xi(t)$, also observed frequencies are linear functions of ξ and are linearly correlated. The slope of this correlation $\omega_\theta^* = K\omega_r^* + Q$ is independent of the energy of oscillations and is given only by parameters of the system,

$$K = \frac{\omega_\theta \lambda_r \nu - \lambda_\theta}{\omega_r \kappa_r \nu - \kappa_\theta}. \quad (45)$$

The slope of the correlation differs from 3:2, however the observed frequencies are still close to it.

3.4. Numerical results

The equations (16), (17) and (21) were solved numerically using the fifth-order Runge-Kutta method with an adaptive step size. One of the solutions is shown in Figure 4. The top panel of the figure shows the time behavior of the amplitudes of the resonant oscillations. Since energy of the system is constant, amplitudes are anticorrelated and the two modes are continuously exchanging energy between each other. The middle and the bottom panels show the two observed frequencies that are mutually correlated. They are also correlated to one of the amplitudes. The frequency ratio varies with time and it differs from the exact 3:2 ratio, however, it always remains very close to it. Our numerical solution is in agreement with the general results obtained analytically in the previous section.

4. Conclusions

Although this paper was originally motivated by observations and models connected to high-frequency QPOs, our results are very general and can be applied to any system with governing equations of the form (1) and (2).

The main result of the calculations is our prediction of low-frequency modulation of the amplitudes and frequencies of oscillations. The characteristic timescale of the modulation is approximately given by equation (44).

Because of the generality of our approach this fact have an interesting consequences in the context of QPO nature of which are unknown. Our result can be summarized in the following way: If the two quasiperiodic oscillations observed close to 3:2 ratio are produced by the autoparametric resonance the frequencies and amplitudes of oscillations should be periodically modulated. This modulation appears as a separate peak at the modulation frequency and as sidebands to the main (linear) oscillation. In a separate paper by Horák et al. (2004) we pointed to possible connection of this modulation with the ‘normal branch oscillations’ (NBOs) that are often present together with QPOs. Specifically, we suggest that the correlation between the higher frequency and the lower amplitude, evident in Figure 4, is the same as was recently reported in Sco X-1 by Yu et al. (2001). We note that similar behavior was recently observed also in the galactic black-hole candidate XTE J1550-564 (Yu et al. 2002).

Acknowledgements. It is a pleasure to thank Vladimír Karas, Marek Abramowicz, Wlodek Kluźniak, Paola Rebusco, Michal Bursa and Michal Dovčiak for helpful discussions. This work was supported by the GACR grant 205/03/0902 and GAUK grant 299/2004.

References

Abramowicz M.A., Bulik T., Bursa M., Kluźniak W., 2002, *A&A*, 404, L21
 Abramowicz M.A., Karas V., Kluźniak W., Lee W.H., Rebusco P., 2003, *PASJ*, 55, 467
 Abramowicz M.A., Kluźniak W., 2001, *A&A*, 374, L19
 Abramowicz M.A., Kluźniak W., 2003, *GRGr*, 35, 69

Abramowicz M.A., Kluźniak W., Stuchlík S., Török G., 2004, *astro-ph/0401464*
 Horák J., Abramowicz M.A., Karas V., Kluźniak W., 2004, *PASJ*, in press
 Horák J., 2005, Doctoral thesis
 Karas V., 1999, *PASJ*, 51, 317
 Kato S., 2003, *PASJ*, 55, 801
 Kato S., 2004, *PASJ*, 56, 559
 Kluźniak W., Abramowicz M.A., 2001, *Acta Phys. Pol. B*, B32, 3605
 Lai D., 1999, *ApJ*, 524, 1030
 Li Li-Xin, Narayan R., 2004, *ApJ*, 601, 414
 Nayfeh A.H., 1973, ‘Perturbation methods’ (John Wiley & sons, New York)
 Nayfeh A.H., Mook D.T., 1979, ‘Nonlinear oscillations’ (John Wiley & sons, New York)
 Rebusco P., 2004, *PASJ*, 56, 553
 Remillard R.A., Muno M.P., McClintock J.E., Orosz J.A., 2002, *ApJ*, 580, 1030
 Rezzolla L., Yoshida S’i., Zanotti O., 2003, *MNRAS*, 344, 978
 Schnittman J.D., Bertschinger E., 2004, *ApJ*, 606, 1098
 Titarchuk L., 2002, *ApJ*, 578, L71
 Yu W., van der Klis M., Jonker P.G., 2001, *ApJ*, 559, L29
 Yu W., van der Klis M., Fender R.P., 2002, in *New Views on microquasars*, eds. Ph. Durouchoux et al. (Center for Space Physics: Kolkate), p. 72